Highly Scalable ZIF-Based Mixed-Matrix Hollow Fiber Membranes for Advanced Hydrocarbon Separations

Chen Zhang, Kuang Zhang, Liren Xu, Ying Labreche, Brian Kraftschik, and William J. Koros
School of Chemical & Biomolecular Engineering, Georgia Institute of Technology, Atlanta, GA 30332

DOI 10.1002/aic.14496
Published online May 29, 2014 in Wiley Online Library (wileyonlinelibrary.com)

ZIF-8/6FDA-DAM, a proven mixed-matrix material that demonstrated remarkably enhanced C_3H_6/C_3H_8 selectivity in dense film geometry, was extended to scalable hollow fiber geometry in the current work. We successfully formed dual-layer ZIF-8/6FDA-DAM mixed-matrix hollow fiber membranes with ZIF-8 nanoparticle loading up to 30 wt % using the conventional dry-jet/wet-quench fiber spinning technique. The mixed-matrix hollow fibers showed significantly enhanced C_3H_6/C_3H_8 selectivity that was consistent with mixed-matrix dense films. Critical variables controlling successful formation of mixed-matrix hollow fiber membranes with desirable morphology and attractive transport properties were discussed. Furthermore, the effects of coating materials on selectivity recovery of partially defective fibers were investigated. To our best knowledge, this is the first article reporting successful formation of high-loading mixed-matrix hollow fiber membranes with significantly enhanced selectivity for separation of condensable olefin/paraffin mixtures. Therefore, it represents a major step in the research area of advanced mixed-matrix membranes. © 2014 American Institute of Chemical Engineers *AIChE J*, 60: 2625–2635, 2014

Keywords: propylene/propane, zeolitic imidazolate frameworks, mixed-matrix membrane, hollow fiber membrane, advanced gas separation

Introduction

Permselective membranes have been studied extensively as energy-efficient separation devices to either retrofit or replace conventional, energy-intensive gas separation processes such as cryogenic distillation and amine-absorption.[1–3] Polymer membranes with excellent scalability have gained market share for air separation, hydrogen recovery, and natural gas purification businesses;[4,5] however, extending polymer membranes to olefin/paraffin separations is more challenging due to insufficient separation efficiency.[6–10] Mixed-matrix membranes comprising both polymers and inorganic components offer a good compromise to address limitations of either of the individual components.[3,11] The potential economic scalability of mixed-matrix membranes makes them attractive when compared with supported zeolite membranes, metal-organic frameworks (MOFs) or zeolitic imidazolate frameworks (ZIFs) membranes,[12] facilitated transport membranes,[13,14] and potentially even carbon molecular sieve (CMS) membranes.[15,16]

Research on mixed-matrix membranes begun in the late 1980s and has received increasing attention,[17–24] especially with rapidly expanding literature on MOFs and ZIFs since 2010.[25–29] While developing membrane materials is a very important part of membrane research, processing membrane materials into practical geometries constitutes another critical aspect.[30] Unfortunately, the majority of published research on mixed-matrix membranes has been focusing on membrane materials and film fabrication at small scale. Much less efforts have been made to advance mixed-matrix membranes into asymmetric hollow fibers, which is the most practical membrane geometry in terms of membrane packing efficiency. Indeed, only a few articles/patents[31–34] have reported formation of mixed-matrix hollow fibers, and these have only considered particle loading below 20 wt %.

Accordingly, despite its excellent scalability, mixed-matrix membranes have yet evolved into commercially viable devices for large-scale gas separations. First, many technical challenges must be addressed to form mixed-matrix hollow fiber membranes with minimized skin defects and attractive selectivity. While spinning neat polymer hollow fiber membranes is well-understood,[10,35] a framework has not been established to transfer intrinsic selectivity of mixed-matrix materials (usually measured on thick dense films) to asymmetric hollow fibers with defect-free and ultrathin selective layers. Additionally, before the invention of hydrophobic MOFs and ZIFs, mixed-matrix membranes were predominantly based on zeolites that required sophisticated surface modifications to adhere with glassy polymer matrices.[36–38] In most cases, moderate performance enhancements of zeolite-based mixed-matrix membranes did not justify the intensive efforts required to scale-up the materials into hollow fibers.

In our previous study,[19] the particle-matrix interfacial adhesion problem was successfully resolved using hydrophobic ZIF-8 as the dispersed molecular sieve. Remarkably enhanced C_3H_6/C_3H_8 selectivity and C_3H_6 permeability were further observed in ZIF-8/6FDA-DAM mixed-matrix dense

Correspondence concerning this article should be addressed to W. J. Koros at wjk@chbe.gatech.edu.

films, which justified the efforts for scale-up. In a more recent article,[39] we reported formation of defect-free neat 6FDA-DAM hollow fiber membranes with optimized spinning dope compositions and spinning parameters. In the current study, on the basis of successfully developed ZIF-8/6FDA-DAM mixed-matrix dense films and neat 6FDA-DAM hollow fibers, we took the opportunity to bring mixed-matrix membrane into an advanced level by forming highly scalable, high-loading ZIF-8/6FDA-DAM mixed-matrix hollow fiber membranes. Efforts were made to address the involved technical challenges including dispersion of nanoparticles, spinning dope processability, and minimization of fiber skin defects. A systematic empirical approach was developed to formulate spinning dope for ZIF-based mixed-matrix hollow fiber membranes. The effects of spinning parameters and coating materials on transport properties were discussed.

Challenges to Develop Scalable Mixed-Matrix Membrane

We first define desirable characteristics of scalable mixed-matrix hollow fiber membranes and identify technical challenges that must be addressed to form such membranes. Ideally, mixed-matrix hollow fiber membrane should show economically attractive selectivity and permeance that are simultaneously enhanced over the neat polymer membrane. In the meantime, the membrane should be easily and inexpensively processed. More specifically, desirable characteristics of scalable mixed-matrix hollow fiber membrane are illustrated in Figure 1 and listed below. To be "*conceptually feasible*," the mixed-matrix hollow fiber membrane should possess the following basic properties to show consistent selectivity with dense film membrane:

1. Dual-layer hollow fiber with particles only in the sheath (outside) layer.
2. Excellent particle-polymer adhesion.
3. Generally well-dispersed particles with minimal agglomerations.
4. Integral skin layer with minimal skin defects.
5. Uniform fiber wall thickness with porous substrate free of macrovoids.

Additionally, to make the mixed-matrix hollow fiber membranes "*economically attractive*," some additional features that are more challenging must be achieved beyond items (1–5):

6. Generally well-dispersed nano-sized particles with minimal agglomerations.
7. Sufficiently high particle loading to show economically attractive selectivity.
8. Minimized skin thickness (<200–500 nm) to enable higher permeance and minimized sheath layer thickness (<1–5 μm) to minimize membrane material cost.
9. Inexpensive polymer as fiber core layer with excellent inter-layer adhesion between sheath layer and core layer.
10. Hollow fine fibers (fiber outer diameter [OD] < 150–300 μm) collected at high take-up rates (>50 m/min) to achieve higher membrane packing density.

Only a few journal articles and patents have reported successful fabrication of mixed-matrix hollow fiber membranes. Several works explored items (1–5) using commercial polymers.[31–34] The particle loading in these mixed-matrix hollow fibers was typically low (up to 20 wt %) and moderately enhanced selectivity was achieved for separation of permanent gases (e.g., CO_2/CH_4 and O_2/N_2). Few data were reported on separation of highly condensable hydrocarbons (e.g., olefin/paraffin). Due to limited advances in items (1–5), the more advanced items (6–10) have rarely been explored. The major four technical challenges to form high-performance, high-loading mixed-matrix hollow fiber membranes satisfying items (1–10) are discussed below:

The challenge to achieve ideal particle-polymer interface

Ideal particle-matrix interface refers to adsorption of polymer chains on particle surface with interfacial polymer chain packing density identical with the bulk polymer phase.[6] Any deviations may lead to nonidealities and experimental transport properties inconsistent with theoretically predicted values. Inorganic molecular sieves such as zeolites and CMS

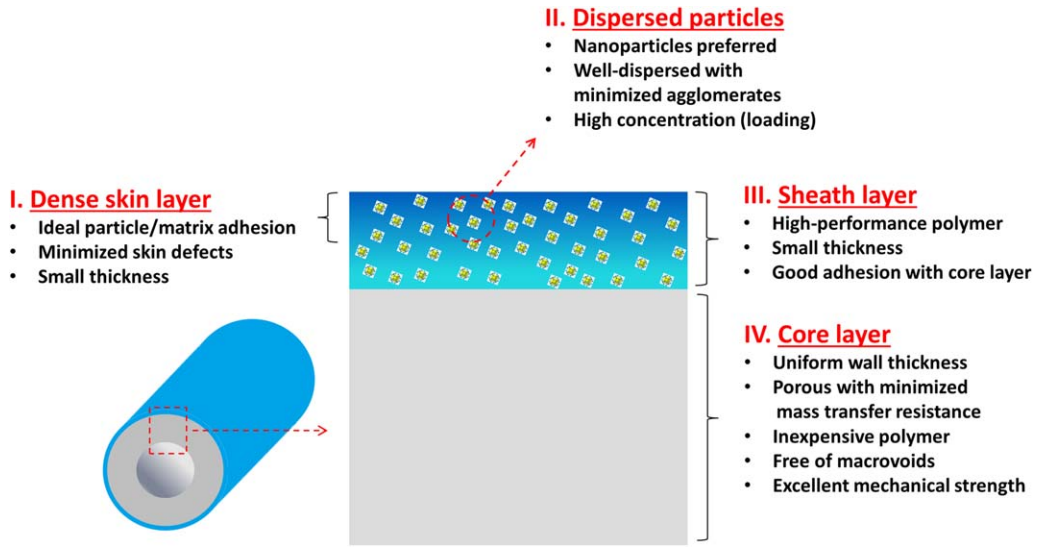

Figure 1. Structural illustration and desirable characteristics of dual-layer mixed-matrix hollow fiber membranes.

[Color figure can be viewed in the online issue, which is available at wileyonlinelibrary.com.]

are not highly compatible with glassy polymers and usually require sophisticated surface treatments to realize good adhesion and enhanced selectivity.[36,37] Detailed discussion of nonideal particle-matrix adhesion and surface treatment techniques can be found elsewhere.[6] It should be noted that this challenge can be successfully addressed by forming mixed-matrix membranes with hydrophobic MOFs and ZIFs that are intrinsically compatible with glassy polymers.[19,40]

The challenge to uniformly disperse nano-sized particles in fiber skin layer

Selective layer of an asymmetric mixed-matrix membrane cannot be thinner than the diameter of a single particle without creating undesirable membrane defects. Accordingly, nano-sized particles are preferred to micron-sized particles for the purpose of minimizing membrane thickness and maximizing membrane permeance. However, nano-sized particles, especially at high concentration, tend to agglomerate more seriously due to their much higher surface energy. The agglomerates in the fiber spinning dope, if sufficiently large, may plug the narrow spinneret channels, thereby leading to ununiform fibers. If present in the fiber skin layer, such agglomerates can also be detrimental to membrane selectivity by introducing skin defects, in the case that the dimension of agglomerates is larger than or comparable with the thickness of fiber skin layer.

Challenges of high-loading mixed-matrix hollow fiber membrane processing

The mixed-matrix hollow fiber membrane described in this article should be differentiated from hollow fiber sorbents,[41] in which the entire fiber wall is porous without a defect-free dense skin layer. For hollow fiber sorbents, breakthrough capacity increases with increasing particle content. For mixed-matrix membrane, selectivity increases with increasing particle loading in the skin layer, and is most attractive for high particle loadings. For both devices, the processability of fiber spinning dope depends on the concentration of solids (polymer and particles). Overly high solid concentration makes the spinning dope difficult to mix homogeneously and extrude from a spinneret.

As a skin layer is unnecessary for hollow fiber sorbents, polymer concentration in its spinning dope can be reduced to ~10 wt % as long as sufficient dope spinnability is retained. Therefore, it is not so challenging to form hollow fiber sorbents with particle loading as high as 70–80 wt %. However, the workable particle loadings of mixed-matrix *hollow fiber membrane* are limited by the requirements on fiber skin integrity. Sufficiently high polymer concentration (usually at least 18–20 wt %, depending on the specific polymer and its Mw) must be used in the spinning dope to form an integral skin with minimal defects and good selectivity. With such high polymer concentration, there is a limit in particle loading of the solidified mixed-matrix hollow fiber membrane, above which the spinning dope would become too difficult to process conveniently at large scale.

In addition to challenges in spinning dope processability, it is also difficult to form thin and defect-free fiber skin layer under high particle loading. Fiber skin formation is a complicated process involving many variables and the effects of particles on skin formation are not yet well-understood. As fiber skin becomes thinner, the probability of fiber skin defects increase dramatically due to over-sized particle agglomerates. While their number can be reduced, particle agglomerates remain a challenge that must be managed during dope extrusion in narrow spinneret channels, owing to high shear rates.[33] Due to the above challenges, successful spinning of high-loading (>20 wt % particles) mixed-matrix hollow fiber gas separation membrane has not been reported previously.

The challenge to balance fiber microscopic properties with macroscopic properties

Among the fiber properties described above, item (2–7) are related to fiber skin formation and can be conveniently referred to as fiber microscopic properties. Conversely, item (1) and (8–10) are referred to as fiber macroscopic properties. Once polymer and particle are selected, these properties will be determined by spinning dope compositions and spinning parameters. In fact, it is difficult to isolate one variable from others as there is a complex interplay between spinning dope rheology, fiber skin vitrification, and phase separation kinetics/thermodynamics.

Often changing one variable may lead to more desirable microscopic properties but will limit the degree of freedom to tune macroscopic properties, and vice versa. For example, longer air gap residence time and cooler quench batch will help to achieve more desirable sheath/core inter-layer adhesion.[42] However, this will inevitably increase fiber skin thickness and limit the maximum fiber take-up speed and minimum fiber OD. For neat polymer hollow fiber membrane, this conflict may be conveniently resolved by optimizing spinning dope composition (such as adding $LiNO_3$ and increasing volatile component concentration) and spinning parameters (such as increasing spinneret temperature). However, for mixed-matrix hollow fiber membranes, especially at higher particle loading, fiber skin integrity is more sensitive to changes in these variables. Accordingly, the "window" allowed to tailor fiber skin thickness and control fiber skin integrity is narrower, and it is more challenging to obtain simultaneously desired fiber microscopic and macroscopic properties.

Experimental

Materials synthesis

ZIF-8 nanoparticles (average radius ~46 nm) were synthesized based on the procedure reported by Cravillon et al.[43]; however, in much larger quantity. 29.4 g $Zn(NO_3)_2{\cdot}6H_2O$ and 32.4g 2-methylimidazole were each dissolved in 2-L methanol. The molar ratio of Zn/MeIM/MeOH was 1:4:1000. The latter solution was poured into the former solution under stirring with a magnetic bar. Stirring was stopped after mixing. After 24 h, the white solids were separated from the dispersion by centrifugation, followed by extensive washing with methanol.

6FDA-DAM polyimide (Mw = 192 kDa) was synthesized using a step growth polymerization method with details described elsewhere.[44] The monomers 6FDA (2,2-bis (3,4-carboxyphenyl) hexafluoropropane dianhydride) and DAM (diaminomesitylene) were purchased from Sigma-Aldrich and purified by sublimation before polymerization.

Preparation of mixed-matrix sheath spinning dope

Mixed-matrix hollow fiber membranes are conventionally formed as dual-layer hollow fibers instead of simpler single-

layer hollow fibers.[31–33] The dual-layer configuration allows independent optimization of fiber skin layer properties and fiber spinnability. Additionally, consumption of expensive molecular sieves can be limited to fiber skin layer where sorption-diffusion-based separation takes place.

Two spinning dopes (core spinning dope and sheath spinning dope) were used to spin dual-layer ZIF-8/6FDA-DAM mixed-matrix hollow fiber membranes in this study. The core spinning dope contained polymer, solvents, non-solvents and was free of ZIF-8 particles. *N*-Methyl-2-pyrrolidone (NMP) and tetrahydrofuran (THF) were used as solvents. Ethanol was used as the non-solvents. The core spinning dope was prepared following the conventional dope preparation technique, which can be found elsewhere.[35] Lithium nitrate ($LiNO_3$) was added in the core spinning dope to improve dope spinnability and accelerate phase separation.

The sheath spinning dope contained ZIF-8 nanoparticles, 6FDA-DAM polyimide, solvents (NMP and THF), and non-solvent (ethanol). This research has identified a valuable approach to form ZIF-based mixed-matrix hollow fiber membranes with minimal particle agglomerations by avoidance of drying ZIF particles before mixing with other components in the sheath spinning dope. After being dried, either under atmosphere or vacuum with or without heat, nano-sized ZIF/MOF particles tend to exist as agglomerates and are very difficult to redisperse in solvents even with strong sonication.[45]

The mixed-matrix sheath spinning dope was prepared with the following procedure. 6FDA-DAM polyimide was dried under vacuum at 100°C for at least 12 h to remove condensables. 15 wt % of the total dried polyimide was dissolved in 30 wt % of the total solvents to form a dilute "priming" dope.[31] After being washed with methanol, ZIF-8 particles (without being dried) were washed with NMP overnight to extract residual methanol from the particles. After the NMP/methanol mixture was separated from the ZIF-8 particles by centrifuge, non-solvent (ethanol) and 70 wt % of the total solvents were added to the centrifuge vials. After being shaken overnight, the slurry was transferred from the centrifuge vials to a sealed 400-mL glass jar and sonicated for at least 1 h using a sonication bath (Elmasonic P30H). Sonication horn was avoided due to possible Ostwald ripening effects that may undesirably change particle dimension and porosity.[46] After ZIF-8 nanoparticles were redispersed, the priming dope was added under constant stirring. After the dope appeared to be homogeneous, remaining (85 wt %) of the total dried polyimide was added under constant stirring. Finally, the jar was sealed and placed on a rolling mixer for at least 2 weeks to ensure that a viscous and homogeneous white paste was formed.

Spinning of hollow fiber membranes

Dual-layer ZIF-8/6FDA-DAM mixed-matrix hollow fiber membranes were formed using the dry-jet/wet-quench fiber spinning technique with a composite spinneret using the setup described previously.[42] To be compared with our previous work on ZIF-8/6FDA-DAM mixed-matrix dense film membranes,[19] two batches of mixed-matrix hollow fibers were spun at ZIF-8 loading of 17 and 30 wt % (in solidified fiber sheath layers), which were close to particle loadings of dense film DAMZ_1 (16.4 wt % ZIF-8) and DAMZ_2 (28.7 wt % ZIF-8), respectively.

The sheath dope, core dope, and bore fluid (90 wt % NMP/10 wt % H_2O) were delivered to the spinneret with controlled flow rates by Isco syringe pumps. The spinning was carried out at desired temperature by heating the entire system including the dope delivery pumps, tubing, dope filters, and spinneret using multiple heating tapes controlled by temperature controllers. The dopes and bore fluid were co-extruded through an adjustable air gap into the water quench bath (height = 1 m), passed over a Teflon guide in the quench bath and collected on a polyethylene rotating take-up drum (diameter = 0.32 m). The take-up drum was partially immersed in a separate water bath at room temperature. The fiber take-up rate used in this research ranged from 5 to 50 m/min. Once cut off from the take-up drum, the dual-layer mixed-matrix fibers were soaked sequentially in at least four separate water baths for 3 days to remove residual organic solvents, and then solvent exchanged with sequential 1 h baths of methanol and hexane. After air-drying in a fume hood for 1 h, the fibers were dried in a vacuum oven at 120°C for ~3 h to remove residual solvents in the fiber as well as to activate ZIF-8. The obtained fibers are referred to as as-spun fibers.

Hollow fiber post-treatments

The surface of as-spun fibers was coated with polydimethylsiloxane (PDMS) and/or polyaramid to seal fiber skin defects, if any existed. To coat the fiber surface with PDMS, the as-spun fibers were contacted with a solution of 2 wt % PDMS (Sylgard® 184, Dow Corning) in iso-octane. After 30 min, the solution was drained and residual iso-octane was removed from the fibers by degassing the fiber at 80°C overnight in a vacuum oven. The obtained fibers are referred to as PDMS-coated fibers.

To coat the fiber surface with both PDMS and polyaramid,[47] the as-spun fibers were contacted with a solution of 0.2 wt % diethyltoluene diamine (DETDA) in iso-octane for 30 min and the solution was drained. The fibers were then further contacted with a second solution of 0.2 wt % trimesoyl chloride (TMC) and 2 wt % PDMS in iso-octane for 30 min and the solution was drained. As the DETDA-impregnated fiber was brought contact with the TMC/PDMS solution, polycondensation occurred between the diamine (DETDA) and the crosslinker (TMC). As a result, crosslinked polyaramid was formed within the network of PDMS on fiber surface. Residual iso-octane was removed by degassing the fibers at 80°C overnight in a vacuum oven. The obtained fibers are referred to as PDMS/polyaramid-coated fibers.

Characterization

Permeation measurements of hollow fiber membranes were performed at 35°C using the constant volume method. A detailed description of constructing hollow fiber membrane modules and permeation testing can be found elsewhere.[48] Permeation of C_3H_6/C_3H_8 was done with mixed-gas feed (50/50 vol %) while O_2/N_2 was done with single-gas feeds. The upstream pressure was ~29.4 psia (~0.2 MPa) for O_2/N_2 permeation; and was ~20 psia (~0.14 MPa) for C_3H_6/C_3H_8 permeation. For mixed-gas measurements, permeate compositions were analyzed with a Varian-450 gas chromatograph. The stage cut was kept less than 1% to avoid concentration polarization. Scanning electron microscopy (SEM) imaging was done on a LEO 1530 field emission scanning electron microscope (LEO Electron Microscopy, Cambridge, UK). Elemental analysis of the

mixed-matrix hollow fiber samples was done by ALS Environmental (Burnaby, Canada). Carbon, nitrogen, hydrogen, and oxygen were analyzed by combustion/IR. Fluorine was analyzed by combustion/IC. Zinc analysis was done by total dissolution.

Results and Discussion

Formation and characterization of ZIF-based mixed-matrix hollow fiber membranes

As a notable advancement over previous research[31] that used micron-sized particles for mixed-matrix hollow fiber spinning, this work formed mixed-matrix hollow fibers with nano-sized particles. As discussed before, ideally an inexpensive commercial polymer should be used to form the fiber core layer. However, as a proof-of-concept, this work used 6FDA-DAM as the core layer polymer to avoid possible sheath-core delamination problem that may complicate the analysis of fiber spinning results.[42]

Formulation of fiber spinning dope is critical to formation of hollow fiber membranes with integral fiber skin and desired transport properties. The conventional "cloud point" technique[49] developed for neat polymer hollow fiber membranes cannot be used to determine dope compositions for mixed-matrix hollow fiber membranes as the added particles would make the dope opaque even in the one-phase region. In the current work, a systematic empirical approach was used to develop dope composition for ZIF-8/6FDA-DAM mixed-matrix hollow fiber membranes, based on the established dope composition of neat 6FDA-DAM hollow fiber membrane reported in our previous study.[39] $LiNO_3$ was originally added in the spinning dope of neat 6FDA-DAM hollow fibers (Table 1) to accelerate phase separation and to improve fiber spinnability; however, it has been shown that it may be hard to control fiber skin integrity in the presence of $LiNO_3$. For dual-layer mixed-matrix hollow fibers, the sheath layer usually comprises a very small amount of the entire fiber. As a result, fiber spinnability and phase separation rate are largely determined by the core spinning dope. In this research, $LiNO_3$ was removed from the sheath spinning dope of mixed-matrix hollow fibers to avoid unnecessary complexities.

Based on the spinning dope of neat 6FDA-DAM hollow fibers, sheath spinning dopes (Table 1) of dual-layer ZIF-8/6FDA-DAM mixed-matrix hollow fibers were developed by making a few adjustments. For mixed-matrix fiber with 17 wt % ZIF-8 loading, the polymer concentration in the sheath spinning dope was fixed around 25 wt % (in this case 26 wt %). Concentration of ZIF-8 in the dope was then determined based on the desired particle loading in the solidified fiber sheath layer. In the meantime, ethanol concentration was reduced so that the total non-solvent (ethanol and ZIF-8) concentration was comparable between these two dopes (15.5 wt % for neat polymer fiber spinning dope vs. 14.2 wt % for mixed-matrix fiber spinning dope). To assist fiber skin formation,[35] THF concentration was increased from 10 to 16 wt %.

The sheath dope composition of dual-layer ZIF-8(30 wt %)/6FDA-DAM mixed-matrix hollow fiber was further developed on the basis of 17 wt % ZIF-8 loading mixed-matrix fiber. It should be noted that such high particle loading has never been reported before in the literature for mixed-matrix hollow fibers. If the polymer concentration was fixed at 26 wt %, ZIF-8 concentration had to be above 11 wt % to reach the desired loading in the solidified sheath layer. This was found to be very challenging to practice as high concentration of polymer, and high concentration of particles would make the dope extremely viscous and difficult to process. To address the processability issue, polymer concentration was reduced to 20 wt %. Therefore, the required ZIF-8 concentration dropped to 8.5 wt %. The resulting sheath spinning dope was still very viscous, but processable. In the meantime, with increasing concentration of ZIF-8, ethanol concentration was decreased to 7.5 wt %. As reducing polymer concentration tend to produce more defective fiber skin, THF concentration was dramatically increased from 16 to 44 wt % to aid fiber skin formation.

Mixed-matrix hollow fibers with 17 and 30 wt % ZIF-8 share the same dope composition for the core spinning dope. A relatively low polymer concentration (20.5 wt %) was used to obtain a more open substrate with minimal mass transfer resistance, and also to reduce the material cost of membrane formation. $LiNO_3$ was added to the core spinning dope to improve dope spinnability and accelerate nascent fiber phase separation. As shown in Table 2, a wide range of spinning parameters was used by varying dope flow rates, air gap height, and quench bath temperature. As particle agglomerations may be more serious at higher particle concentration, cooler quench bath (12–25°C) was used for 30 wt % ZIF-8 loading mixed-matrix fiber. Lower quench batch temperature may produce thicker and less defective skin. Spinning parameters of the spinning state showing the highest fiber selectivity are shown in parentheses.

SEM images (fiber overview, fiber substrate, fiber skin side view, and fiber skin top view) of dual-layer ZIF-8/6FDA-DAM mixed-matrix hollow fibers are shown in Figure 2, column B (17 wt % ZIF-8) and C (30 wt % ZIF-8), respectively. SEM images of single-layer neat 6FDA-DAM hollow fiber membranes are shown in Figure 2, column A for reference. The mixed-matrix fibers had generally attractive macroscopic properties with an OD$\sim$400 μm and sheath

Table 1. Spinning Dope Compositions (wt %) of Dual-Layer ZIF-8/6FDA-DAM Mixed-Matrix Hollow Fiber Membranes

	Sheath Spinning Dope			
Component	Neat Polyimide	17 wt % ZIF-8	30 wt % ZIF-8	Core Spinning Dope
6FDA-DAM	25	26	20	20.5
NMP	49.5	43.8	20	48
THF	10	16	44	10
Ethanol	12	9	7.5	15
$LiNO_3$	3.5	0	0	6.5
ZIF-8	0	5.2	8.5	0

The dope composition of neat 6FDA-DAM hollow fiber membranes is shown for reference.

Table 2. Spinning Parameters of Dual-Layer ZIF-8/6FDA-DAM Mixed-Matrix Hollow Fiber Spinning

Spinning Parameter	17 wt % ZIF-8 fiber	30 wt % ZIF-8 fiber
Sheath dope flow rate (cc/h)	15–30 (15)	15–30 (15)
Core dope flow rate (cc/h)	150–300 (150)	150–180 (150)
Bore fluid flow rate (cc/h)	55–100 (55)	55–60 (55)
Quench bath temperature (°C)	25–50 (25)	12–25 (12)
Spinneret temperature (°C)	50–60 (60)	50–60 (60)
Air gap height (cm)	7–30 (10)	2–30 (2)
Take-up rate (m/min)	5–20 (10)	5–20 (10)

Spinning parameters of the spinning state showing the highest fiber selectivity are shown in parentheses.

layer thickness of 7–12 μm. Striking differences were observed for fiber skin top views (Figures 2, A-IV, B-IV, and C-IV). While the skin surface of neat 6FDA-DAM fiber appeared to be completely smooth without any observable features, the surface of the mixed-matrix fiber skin displayed many small "nodules" with dimensions close to the size of individual ZIF-8 nanoparticles (diameter ~100 nm). In addition, these "nodules" seem to become more densely packed as particle loading increased from 17 to 30 wt %.

Many circular sockets with diameter of ~100 nm can be seen in skin side views of mixed-matrix fibers (Figure 2, B-III & C-III). Such morphology was not observed for neat 6FDA-DAM fiber without ZIF-8 nanoparticles (Figure 2, A-III). We hypothesize that formation of these sockets was due to ZIF-8 nanoparticles "popping out" from the fiber upon aggressive sample fracturing in liquid nitrogen and, therefore, is not an indication of fiber skin defects. It should be noted that due to these sockets, the transition from fiber dense skin and the underneath porous region was unclear. As a result, it was hard to unambiguously estimate skin layer thickness of mixed-matrix hollow fiber membranes simply based on SEM imaging. The presence of ZIF-8 particles in the fiber sheath layer was further confirmed by elemental analysis of hollow fiber sheath layers. As shown in Figure 3, experimental Zn weight fractions agreed very well with the theoretical values.

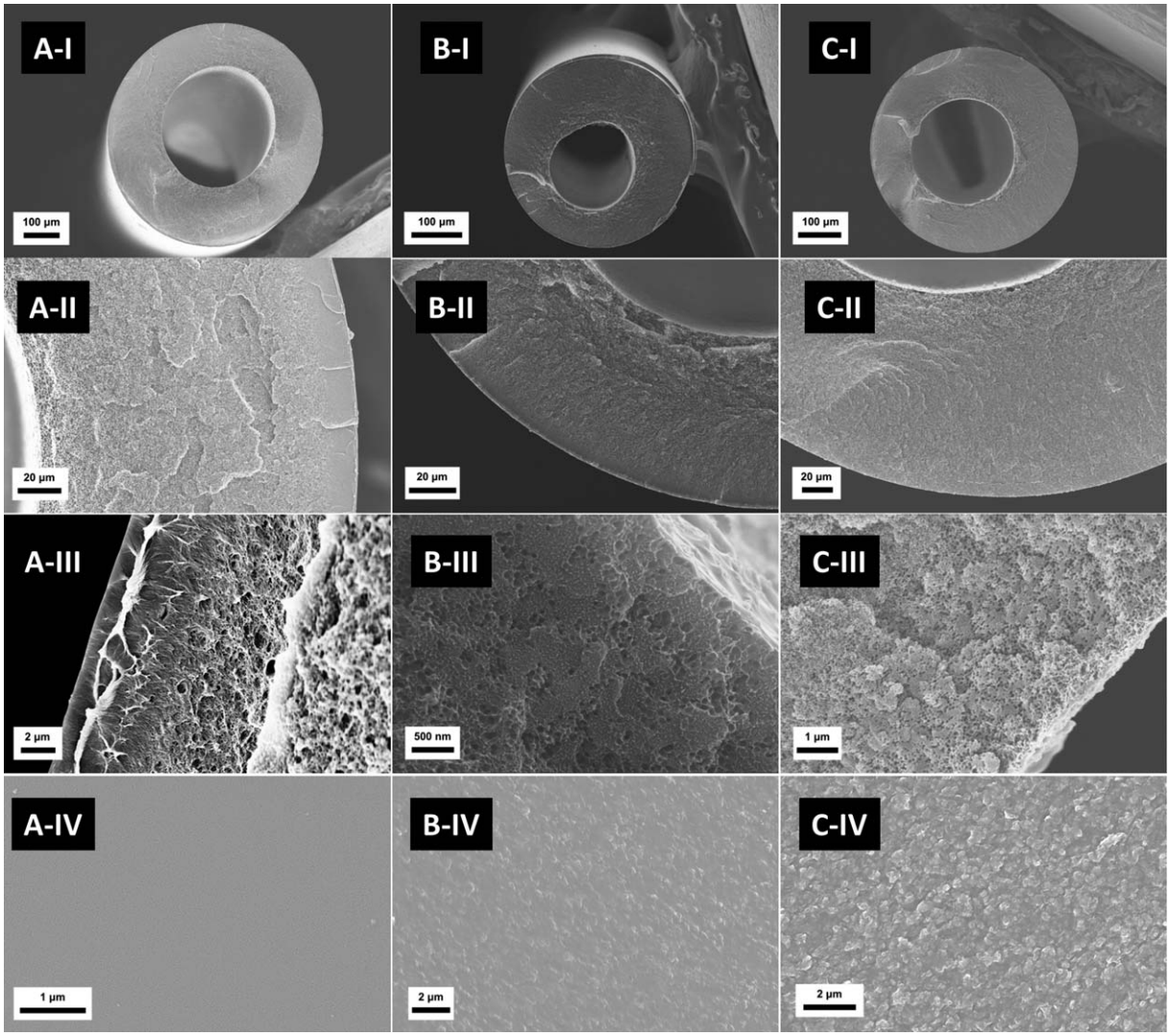

Figure 2. SEM images of hollow fiber membranes.

A: Single-layer neat 6FDA-DAM hollow fiber membrane; B: Dual-layer ZIF-8 (17 wt %)/6FDA-DAM mixed-matrix hollow fiber membrane; C: Dual-layer ZIF-8 (30 wt %)/6FDA-DAM mixed-matrix hollow fiber membrane. I: fiber overview; II: fiber substrate; III: fiber skin layer side view; and IV: fiber skin layer top view.

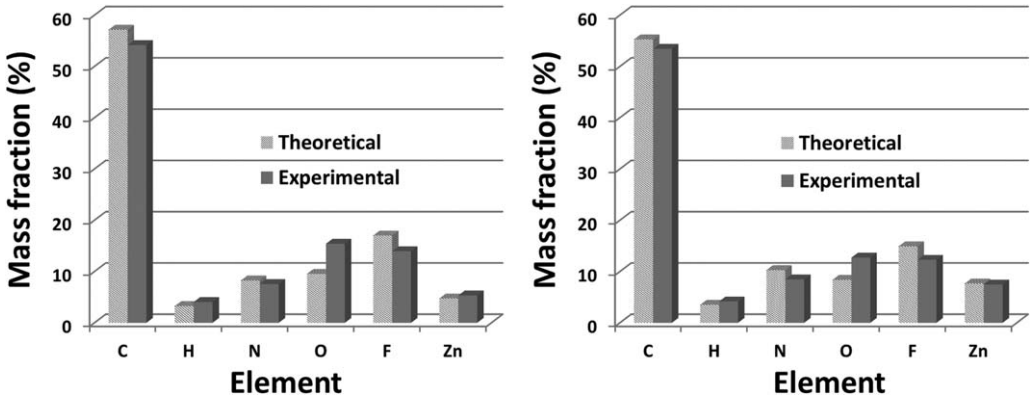

Figure 3. Elemental analysis results of sheath layers of ZIF-8/6FDA-DAM mixed-matrix hollow fiber membranes.

Left: 17 wt % ZIF-8 loading mixed-matrix fiber; Right: 30 wt % ZIF-8 loading mixed-matrix fiber.

Transport properties of ZIF-based mixed-matrix hollow fiber membranes

By varying the spinning parameters listed in Table 2, 10–12 different states were each obtained for 17 and 30 wt % loading mixed-matrix fibers. The quality of as-spun fibers was first examined by O_2/N_2 single-gases permeation. Those states showing highest O_2/N_2 selectivities were further evaluated for C_3H_6/C_3H_8 separation with results shown in Table 3. Permeation data of single-layer neat 6FDA-DAM hollow fiber membrane are shown as well for reference.

With added $LiNO_3$ in the core spinning dope, spinnability of dual-layer mixed-matrix hollow fibers was excellent. With 50°C quench batch, dual-layer mixed-matrix fibers can be collected continuously at drawing speed as high as 50 m/min, which resulted in fine fibers with OD as small as ~260 μm. However, initial examination with O_2/N_2 single-gases permeation suggested that fibers spun with 50°C quench batch were defective with much lower selectivities. On the contrary, those states spun using cooler quench batch and lower drawing speed (10 m/min) generally had better selectivities. This was probably due to the thicker fiber skin formed with longer air gap residence time and slower phase separation in the cooler quench bath.

Spinning parameters of the state demonstrating highest O_2/N_2 selectivity are shown in parentheses of Table 2. For 17 wt % ZIF-8 loading mixed-matrix fiber, highest O_2/N_2 selectivity was achieved with air gap of 10 cm, drawing speed of 10 m/min and 25°C quench bath. An O_2/N_2 selectivity of 4.5 was obtained for the as-spun fiber, which was slightly higher than the value (4.0) of mixed-matrix dense film with similar loading (DAMZ_1). The fiber skin thickness (~2.7 μm) was estimated using O_2 permeability of DAMZ_1 (186 Barrer)[19] and permeance of the as-spun mixed-matrix fiber (69.3 GPU). C_3H_6/C_3H_8 mixed-gas permeation showed that the as-spun fiber had good C_3H_6/C_3H_8 separation performance with C_3H_6 permeance of 2.4 GPU and C_3H_6/C_3H_8 selectivity of 16.5. It was surprising, yet obviously desirable to see, that the C_3H_6/C_3H_8 selectivity of the mixed-matrix fiber exceeded the value (13.7) of mixed-matrix dense film at similar loading (DAMZ_1). We hypothesize that this was due to better particle dispersion in hollow fibers using lab-synthesized ZIF-8 particles, which were less susceptible to agglomerations than a commercially available ZIF-8 sample used in our previous dense film work. Polymer chain orientations may also contributed to the increased selectivity, which resulted from extensional forces applied on the nascent fiber. In any case, this suggested successful formation of high-quality mixed-matrix fiber with minimal skin defects. Coating fiber surface with PDMS slightly enhanced C_3H_6/C_3H_8 selectivity to 17.7 with a minor drop of C_3H_6 permeance to 2.2 GPU. This indicates that tiny defects still existed, although apparently their impacts on C_3H_6/C_3H_8 selectivity were minimal. To our best knowledge, this was among the few studies that as-spun mixed-matrix hollow fiber membranes showed consistent selectivity with the mixed-matrix dense film membranes. It was also the first time that mixed-matrix hollow fiber membrane showed enhanced selectivity for separation of condensable olefin/paraffin mixtures.

For 30 wt % ZIF-8 loading mixed-matrix fiber, highest O_2/N_2 selectivity (4.0) was achieved at quench bath temperature of 12°C. Those states spun under 25°C quench bath temperature generally showed lower selectivities. The optimal state was further taken for C_3H_6/C_3H_8 mixed-gas permeation. Surprisingly, the C_3H_6/C_3H_8 selectivity of this state was only 6.6, which was significantly lower than the value (18.1) of mixed-matrix dense film membrane with similar loading (DAMZ_2). After coating the fiber surface with PDMS, O_2/N_2 selectivity slightly increased to 4.2 with O_2 permeance dropped by 20%. In the meantime, C_3H_6 permeance was reduced by 40% with C_3H_6/C_3H_8 selectivity increased to 16.4, which was still lower than the dense film selectivity. That is to say, PDMS coating was not effective to fully recover C_3H_6/C_3H_8 selectivity of 30 wt % ZIF-8 loading mixed-matrix fiber. Also, as the fiber was partially defective at 30 wt % loading, reliable estimation of fiber skin layer thickness was not possible.

Effect of coating materials on selectivity recovery of partially defective fibers

It is hypothesized that the inadequacy of PDMS as a coating material to restore hollow fiber C_3H_6/C_3H_8 selectivity was due to their poorly matched C_3H_8 permeability. The effectiveness of a coating material to seal fiber skin defects depends on the relative permeability of the slower permeating component in the coating material and the membrane material comprising the fiber skin. In the case that the coating material is several orders of magnitude more permeable than the membrane, it may not be effective to slow down unselective Knudsen diffusion in fiber skin defects.

Table 3. Permeation Results of Hollow Fiber Membranes

Fiber	Permeance (GPU)		Selectivity	
	O_2	C_3H_6	O_2/N_2	C_3H_6/C_3H_8
Single-layer neat 6FDA-DAM hollow fiber membrane				
As-spun fiber	87.5	9.3	4.2	8.0
PDMS-coated fiber	78.0	7.3	4.2	8.5
PDMS/polyaramid-coated fiber	6.3	0.38	6.3	16.3
Dual-layer ZIF-8 (17 wt %)/6FDA-DAM mixed-matrix hollow fiber membrane				
As-spun fiber	69.3	2.4	4.5	16.5
PDMS-coated fiber	66.5	2.2	4.5	17.7
PDMS/polyaramid-coated fiber	25.3	0.68	7.7	21.1
Dual-layer ZIF-8 (30 wt %)/6FDA-DAM mixed-matrix hollow fiber membrane				
As-spun fiber	73.9	10.1	4.0	6.6
PDMS-coated fiber	59.5	6.0	4.2	16.4
PDMS/polyaramid-coated fiber	7.3	0.27	7.0	27.5

Permeation of O_2/N_2 was done with single gases at 35°C and 29.4 psia (~0.2 MPa) upstream pressure. Permeation of C_3H_6/C_3H_8 was done with 50/50 vol % mixed-gas at 35°C and 20 psia (~0.14 MPa) upstream pressure. 1GPU = 3.348×10^{-10} mol/m^2 s Pa.

Permeability data in PDMS and 6FDA-DAM polyimide are plotted in Figure 4 with penetrant molecular size. Permeabilities of H_2, O_2, N_2, CH_4, C_3H_6, and C_3H_8 in 6FDA-DAM were measured at 35°C.[19,50] Permeability data of H_2, O_2, N_2, and CH_4 in PDMS were reported by Freeman and coworkers at 35°C.[51] Permeabilities of C_3H_6 and C_3H_8 in PDMS were measured by Tanaka et al. at 50°C.[52] Permeabilities of *n*-C_4H_{10} and *iso*-C_4H_{10} were calculated based on permeation data at 100°C and permeation activation energy.[53,54] Permeation in rubbery PDMS is controlled by solubility, and permeability increases as the penetrant becomes more condensable. On the contrary, permeation in glassy 6FDA-DAM is controlled by diffusion, and permeability decreases with increasing penetrant molecular size. Consequently, the permeability ratio between PDMS and 6FDA-DAM increases dramatically as the penetrant molecule becomes larger and more condensable. For example, the ratio of H_2 permeability is only ~3, while the ratio of *n*-C_4H_{10} is over 6×10^4.

Figure 5 further shows the effectiveness of PDMS to seal fiber skin defects for separation of O_2/N_2, CO_2/CH_4, C_3H_6/C_3H_8, and *n*-C_4H_{10}/*iso*-C_4H_{10}. The *X* axis is the fractional area (percentage) of fiber skin defects. The *Y* axis is the normalized selectivity of the coated fiber relative to the intrinsic selectivity of the fiber skin material. Calculations were done with the resistance model suggested by Henis and Tripodi.[55]

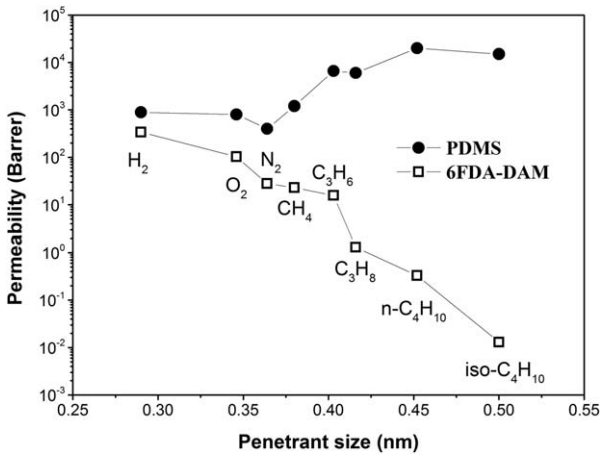

Figure 4. Permeability data in PDMS and 6FDA-DAM. 1 Barrer = 3.347×10^{-16} mol m/m^2 s Pa.

Clearly, as a coating material to seal fiber skin defects, PDMS is not as effective for separation of highly condensable hydrocarbons as for separation of permanent gases. For example, assuming 0.1% fiber skin defects, selectivities of O_2/N_2, CO_2/CH_4 were within 95% of the intrinsic selectivity after PDMS coating. Whereas C_3H_6/C_3H_8 and *n*-C_4H_{10}/*iso*-C_4H_{10} selectivities of the PDMS-coated fiber were only less than 30 and 10% of the intrinsic selectivity, respectively. That is to say, it is much more challenging to obtain high-quality hollow fiber membranes that demonstrate desirable hydrocarbon selectivity consistent with dense film membrane. For PDMS-coated 6FDA-DAM hollow fibers, percentage of fiber skin defects has to be below 2×10^{-5} to show defect-free (90%) C_3H_6/C_3H_8 selectivity. For *n*-C_4H_{10}/*iso*-C_4H_{10}, the required percentage is even lower (8×10^{-8}).

The above analysis indicates that coating materials that are much less permeable than PDMS must be used to effectively slow down Knudsen diffusion of hydrocarbons in fiber skin defects. Polyaramids can be conveniently formed *in situ* on hollow fiber surface, usually by reacting aromatic di/tri-amine and di/tri-acryl chloride monomers. Polyaramids have been used as membrane coating materials in several studies. The monomers were believed to be slim enough to diffuse

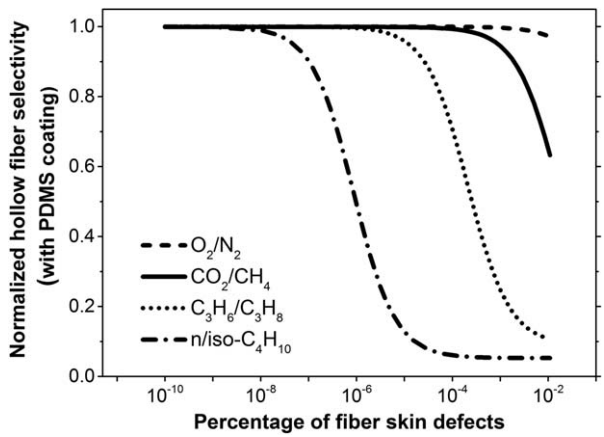

Figure 5. Normalized selectivity of PDMS-coated 6FDA-DAM hollow fiber vs. percentage of fiber skin defects.

It is assumed that PDMS fills the defects as well as forms a continuous layer on top of the fiber surface.

into and polymerize inside smaller defects, providing small interstitial seals that cannot be realized by bulkier PDMS. Additionally, polyaramids are glassy polymers with rigid chains, and tend to be much less permeable than PDMS. Based on the analysis in Figure 5, we believe that glassy polyaramid should be more effective than rubber PDMS to recover hydrocarbon selectivity of partially defective hollow fiber membranes.

To study polyaramid's effectiveness, the as-spun fibers were coated with a blend of PDMS and polyaramid following the procedure described in the experimental section. PDMS was retained in the coating as it may be able to seal large-sized defects that *in situ* polymerized polyaramid cannot entirely cover. The PDMS/polyaramid-coated fibers were tested for permeation and the results were compared with as-spun fibers and PDMS-coated fibers (Table 3). After the partially defective 30 wt % ZIF-8 loading mixed-matrix fiber was coated with PDMS/polyaramid, C_3H_6/C_3H_8 selectivity was dramatically enhanced from 16.4 to 27.5, which was ~50% higher than the intrinsic value of the dense film (DAMZ_2).[19] This suggested that polyaramid was indeed more effective than PDMS to recover the fiber's C_3H_6/C_3H_8 selectivity.

For comparison purposes, the as-spun neat 6FDA-DAM fiber and as-spun 17 wt % ZIF-8 loading mixed-matrix fiber were also coated by PDMS/polyaramid and tested for permeation. It should be noted that these fibers were close to being defect-free and polyaramid coating was not required to show selectivity consistent with dense films. As shown in Table 3, selectivities were again increased above the dense film value. This indicates that the polyaramid was intrinsically more selective than the underlying fiber. In any case, C_3H_6/C_3H_8 selectivity increased nicely with increasing ZIF-8 loading when comparing PDMS/polyaramid-coated fibers. This was consistent with the trend observed for dense films (Figure 6) and suggested that adding ZIF-8 indeed enhanced C_3H_6/C_3H_8 selectivity of the hollow fiber membrane.

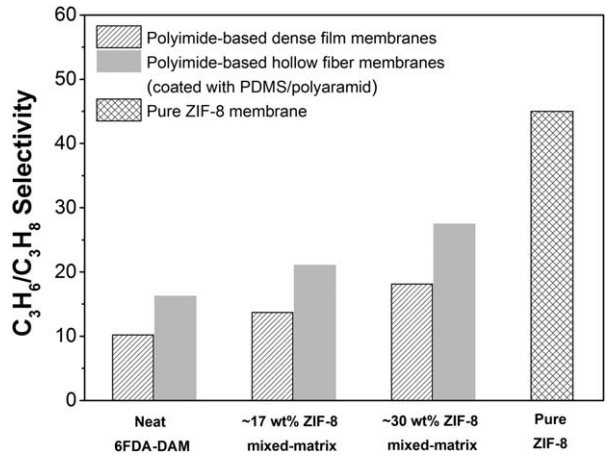

Figure 6. Comparison of C_3H_6/C_3H_8 selectivities of polyimide-based dense films and hollow fibers (coated with PDMS/polyaramid).

Permeation measurements of dense films and hollow fibers were done under the same conditions: 50/50 C_3H_6/C_3H_8 binary feed mixture at 20 psia (~0.14 MPa) and 35°C. The C_3H_6/C_3H_8 selectivity measured by Kwon and Jeong[12] (50/50 C_3H_6/C_3H_8 binary feed mixture at ~0.1 MPa and ~35°C) on a supported ZIF-8 membrane is also shown for comparison.

Due to strong hydrogen bonding, polyaramids are usually quite impermeable.[56] The drastically reduced permeance of PDMS/polyaramid-coated fibers (Table 3) indicated that the particular polyaramid (based on DETDA and TMC) added substantial mass transfer resistance to permeation. That is to say, the chemistry of polyaramid and coating conditions must be optimized so that membrane permeance is not significantly compromised, which is however, not within the scope of the current work. In any case, as a proof-of-concept, this article successfully proves that it was possible, although challenging, to realize attractive olefin/paraffin selectivity enhancements in scalable mixed-matrix hollow fiber membranes with high particle loading.

Comparison with supported ZIF-8 membranes

To take advantage of ZIF-8's attractive molecular sieving properties[50,57] for energy-efficient C_3H_6/C_3H_8 separation, an alternative to mixed-matrix membrane is pure ZIF-8 membrane. Such membranes are usually formed by growing a continuous ZIF-8 layer atop a porous substrate (e.g., porous alumina). Several recent studies[12,58,59] reported fabrication of supported ZIF-8 membranes showing actual mixed-gas C_3H_6/C_3H_8 selectivity of ~30–45 under permeation conditions similar to the current study. Specifically, the result by Kwon and Jeong[12] was plotted in Figure 6 to be compared with ZIF-8-based mixed-matrix hollow fibers. Conversely, a pure component C_3H_6 and C_3H_8 permeation study[60] showed overly optimistic selectivity and productivity results, due to competitive sorption and diffusion factors in actual mixtures such as those studied here and in other supported ZIF-8 membranes.

Compared with supported ZIF-8 membranes, ZIF-8-based mixed-matrix hollow fibers offer the advantage of superior scalability. At 30 wt % ZIF-8 loading, hollow fiber C_3H_6/C_3H_8 selectivity (27.5, Table 3) had started to approach supported ZIF-8 membranes. While C_3H_6 permeance of ZIF-8/6FDA-DAM mixed-matrix hollow fibers are much lower compared with supported ZIF-8 membranes, the difference can be potentially offset by the capability of hollow fiber module to provide much higher membrane area in a given volume. With further optimization of composite hollow fiber spinning techniques, the currently discussed mixed-matrix approach is potentially able to economically deliver attractive C_3H_6/C_3H_8 separation efficiency that is at least competitive with supported ZIF-8 membranes. Formation of ultrahigh ZIF-8 loading (>40 wt %) mixed-matrix hollow fiber membrane is under way and will be reported in our future work; however, many challenges remain to achieve defect-free performance under such high particle loading.

Conclusions

Development of highly scalable, high-loading ZIF-based mixed-matrix hollow fiber membrane was investigated in this study. Technical challenges to realize attractive selectivity enhancements of mixed-matrix materials in hollow fiber geometry were analyzed and discussed with great detail. We developed a systematic empirical approach to formulate spinning dope for ZIF-based mixed-matrix hollow fiber membranes. ZIF-8 nanoparticles were used to form dual-layer ZIF-8/6FDA-DAM mixed-matrix hollow fiber membrane with excellent spinnability and desirable macroscopic properties. The as-spun 17 wt % ZIF-8 loading mixed-matrix fiber was very high quality showing significantly enhanced $C_3H_6/$

C_3H_8 selectivity. While the as-spun 30 wt % ZIF-8 loading mixed-matrix fiber was partially defective, we found that fiber skin defects were effectively sealed by coating fiber surface with a blend of PDMS and polyaramid. Overall, hollow fiber C_3H_6/C_3H_8 selectivity increased with increasing ZIF-8 loading up to 30 wt %, which was in decent consistency with previously reported dense film permeation data.

Unlike most recently published works on mixed-matrix membranes, this article focused on translation of attractive separation performance into a scalable membrane geometry (hollow fiber), which the authors believe are extremely important to advance the concept of mixed-matrix membrane beyond academic research. To our best knowledge, this is the first article reporting successful formation of high-loading mixed-matrix hollow fiber membranes that deliver significantly enhanced selectivity for condensable hydrocarbon mixtures. While substantial efforts are needed in the future to make the membrane eventually meet the requirements of being "*economically attractive*," in this article we have demonstrated that ZIF-based mixed-matrix hollow fiber membranes are indeed "*conceptually feasible*."

Acknowledgment

This publication is based on work supported by Award No. KUS-I1-011-21, made by King Abdullah University of Science and Technology (KAUST).

Literature Cited

1. Baker RW. Future directions of membrane gas separation technology. *Ind Eng Chem Res*. 2002;41(6):1393–1411.
2. Caro J, Noack M. Zeolite membranes—Recent developments and progress. *Microporous Mesoporous Mat*. 2008;115(3):215–233.
3. Koros WJ, Lively RP. Water and beyond: Expanding the spectrum of large-scale energy efficient separation processes. *AIChE J*. 2012; 58(9):2624–2633.
4. Robeson LM. The upper bound revisited. *J Membr Sci*. 2008;320: 390–400.
5. Sanders DF, Smith ZP, Guo R, Robeson LM, McGrath JE, Paul DR, Freeman BD. Energy-efficient polymeric gas separation membranes for a sustainable future: A review. *Polymer*. 2013;54(18):4729–4761.
6. Hoek EMV, Tarabara VV. *Encyclopedia of Membrane Science and Technology*. John Wiley and Sons, New York, 2013.
7. Burns RL, Koros WJ. Defining the challenges for C_3H_6/C_3H_8 separation using polymeric membranes. *J Membr Sci*. 2003;211(2):299–309.
8. Motelica A, Bruinsma OSL, Kreiter R, den Exter M, Vente JF. Membrane retrofit option for paraffin/olefin separation-a technoeconomic evaluation. *Ind Eng Chem Res*. 2012;51(19):6977–6986.
9. Colling CW, Huff GA Jr, Bartels JV. Process Using Solid Permselective Membranes in Multiple Groups for Simultaneous Recovery of Specified Products from a Fluid Mixture. US Patent 6830691B2, 2004.
10. Roman IC, Simmons JW, Ekiner OM. *Method of Separating Olefins from Mixtures with Paraffins*. US Patent 7399897 B2, 2008.
11. Moore TT, Mahajan R, Vu DQ, Koros WJ. Hybrid membrane materials comprising organic polymers with rigid dispersed phases. *AIChE J*. 2004;50:311–321.
12. Kwon HT, Jeong H-K. In situ synthesis of thin zeolitic-imidazolate framework ZIF-8 membranes exhibiting exceptionally high propylene/propane separation. *J Am Chem Soc*. 2013;135(29):10763–10768.
13. Merkel TC, Blanc R, Ciobanu I, Firat B, Suwarlim A, Zeid J. Silver salt facilitated transport membranes for olefin/paraffin separations: Carrier instability and a novel regeneration method. *J Membr Sci*. 2013;447:177–189.
14. Faiz R, Li K. Olefin/paraffin separation using membrane based facilitated transport/chemical absorption techniques. *Chem Eng Sci*. 2012;73(0):261–284.
15. Xu LR, Rungta M, Koros WJ. Matrimid® derived carbon molecular sieve hollow fiber membranes for ethylene/ethane separation. *J Membr Sci*. 2011;380(1–2):138–147.
16. Rungta M, Zhang C, Koros WJ, Xu L. Membrane-based ethylene/ethane separation: The upper bound and beyond. *AIChE J*. 2013; 59(9):3475–3489.
17. Zimmerman CM, Singh A, Koros WJ. Tailoring mixed matrix composite membranes for gas separations. *J Membr Sci*. 1997;137(1–2): 145–154.
18. Vu DQ, Koros WJ, Miller SJ. Mixed matrix membranes using carbon molecular sieves - I. Preparation and experimental results. *J Membr Sci*. 2003;211(2):311–334.
19. Zhang C, Dai Y, Johnson JR, Karvan O, Koros WJ. High performance ZIF-8/6FDA-DAM mixed matrix membrane for propylene/propane separations. *J Membr Sci*. 2012;389(0):34–42.
20. Caro J. Are MOF membranes better in gas separation than those made of zeolites? *Curr Opin Chem Eng*. 2011;1(1):77–83.
21. Li T, Pan Y, Peinemann K-V, Lai Z. Carbon dioxide selective mixed matrix composite membrane containing ZIF-7 nano-fillers. *J Membr Sci*. 2013;425–426(0):235–242.
22. Askari M, Chung TS. Natural gas purification and olefin/paraffin separation using thermal cross-linkable co-polyimide/ZIF-8 mixed matrix membranes. *J Membr Sci*. 2013;444:173–183.
23. Ploegmakers J, Japip S, Nijmeijer K. Mixed matrix membranes containing MOFs for ethylene/ethane separation Part A: Membrane preparation and characterization. *J Membr Sci*. 2013;428(0):445–453.
24. Minelli M, Doghieri F, Papadokostaki KG, Petropoulos JH. A fundamental study of the extent of meaningful application of Maxwell's and Wiener's equations to the permeability of binary composite materials. Part I: A numerical computation approach. *Chem Eng Sci*. 2013;104(0):630–637.
25. Park KS, Ni Z, Cote AP, Choi JY, Huang R, Uribe-Romo FJ, Chae HK, O'Keeffe M, Yaghi, OM. Exceptional chemical and thermal stability of zeolitic imidazolate frameworks. *Proc Natl Acad Sci USA*. 2006;103:10186–10191.
26. Phan A, Doonan CJ, Uribe-Romo FJ, Knobler CB, O'Keeffe M, Yaghi OM. Synthesis, structure, and carbon dioxide capture properties of zeolitic imidazolate frameworks. *Acc Chem Res*. 2010;43:58–67.
27. Zhang K, Lively RP, Zhang C, Chance RR, Koros WJ, Sholl DS, Nair S. Exploring the framework hydrophobicity and flexibility of ZIF-8: From biofuel recovery to hydrocarbon separations. *J Phys Chem Lett*. 2013;4(21):3618–3622.
28. Zhang L, Hu Z, Jiang J. Sorption-induced structural transition of zeolitic imidazolate framework-8: A hybrid molecular simulation study. *J Am Chem Soc*. 2013;135(9):3722–3728.
29. Herm ZR, Bloch ED, Long JR. Hydrocarbon separations in metal–organic frameworks. *Chem Mater*. 2013;26(1):323–338.
30. Koros WJ, Fleming GK. Membrane-based gas separation. *J Membr Sci*. 1993;83(1):1–80.
31. Husain S, Koros WJ. Mixed matrix hollow fiber membranes made with modified HSSZ-13 zeolite in polyetherimide polymer matrix for gas separation. *J Membr Sci*. 2007;288(1–2):195–207.
32. Dai Y, Johnson JR, Karvan O, Sholl DS, Koros WJ. Ultem®/ZIF-8 mixed matrix hollow fiber membranes for CO_2/N_2 separations. *J Membr Sci*. 2012;401–402(0):76–82.
33. Ekiner OM, Kulkarni SS. *Process for Making Hollow Fiber Mixed Matrix Membranes*. US Patent 6663805, 2003.
34. Ismail AF, Kusworo TD, Mustafa A. Enhanced gas permeation performance of polyethersulfone mixed matrix hollow fiber membranes using novel Dynasylan Ameo silane agent. *J Membr Sci*. 2008; 319(1–2):306–312.
35. Clausi DT, Koros WJ. Formation of defect-free polyimide hollow fiber membranes for gas separations. *J Membr Sci*. 2000;167(1):79–89.
36. Lydon ME, Unocic KA, Bae TH, Jones CW, Nair S. Structure-property relationships of inorganically surface-modified zeolite molecular sieves for nanocomposite membrane fabrication. *J Phys Chem C*. 2012;116(17):9636–9645.
37. Shu S, Husain S, Koros WJ. A general strategy for adhesion enhancement in polymeric composites by formation of nanostructured particle surfaces. *J Phys Chem C*. 2007;111(2):652–657.
38. Liu J, Bae T-H, Qiu W, Husain S, Nair S, Jones CW, Chance RR, Koros WJ. Butane isomer transport properties of 6FDA-DAM and MFI-6FDA-DAM mixed matrix membranes. *J Membr Sci*. 2009; 343(1–2):157–163.

39. Xu L, Zhang C, Rungta M, Qiu W, Liu J, Koros WJ. Formation of defect-free 6FDA-DAM asymmetric hollow fiber membranes for gas separations. *J Membr Sci*. 2014;459(0):223–232.
40. Ordonez MJC, Balkus KJ Jr, Ferraris JP, Musselman IH. Molecular sieving realized with ZIF-8/Matrimid mixed-matrix membranes. *J Membr Sci*. 2010;361:28–37.
41. Lively RP, Chance RR, Kelley BT, Deckman HW, Drese JH, Jones CW, Koros WJ. Hollow fiber adsorbents for CO_2 removal from flue gas. *Ind Eng Chem Res*. 2009;48(15):7314–7324.
42. Ma C, Koros WJ. Ester-cross-linkable composite hollow fiber membranes for CO_2 removal from natural gas. *Ind Eng Chem Res*. 2013; 52(31):10495–10505.
43. Cravillon J, Nayuk R, Springer S, Feldhoff A, Huber K, Wiebcke M. Controlling zeolitic imidazolate framework nano- and microcrystal formation: Insight into crystal growth by time-resolved in situ static light scattering. *Chem Mater*. 2011;23(8):2130–2141.
44. Vora RH. *Process of Making a Shaped Article from Intermediate Molecular Weight Polyimide*. US Patent 4933132, 1989.
45. Seoane B, Sebastian V, Tellez C, Coronas J. Crystallization in THF: The possibility of one-pot synthesis of mixed matrix membranes containing MOF MIL-68(Al). *CrystEngComm*. 2013;15(45):9483–9490.
46. Thompson JA, Chapman KW, Koros WJ, Jones CW, Nair S. Sonication-induced Ostwald ripening of ZIF-8 nanoparticles and formation of ZIF-8/polymer composite membranes. *Microporous Mesoporous Mater*. 2012;158:292–299.
47. Ekiner OM, Hayes RA, Manos P. *Reactive Post Treatment for Gas Separation Membrane*. US Patent 5091216, 1992.
48. Vu DQ, Koros WJ, Miller SJ. High pressure CO_2/CH_4 separation using carbon molecular sieve hollow fiber membranes. *Ind Eng Chem Res*. 2002;41(3):367–380.
49. Wallace DW, Staudt-Bickel C, Koros WJ. Efficient development of effective hollow fiber membranes for gas separations from novel polymers. *J Membr Sci*. 2006;278(1–2):92–104.
50. Zhang C, Lively RP, Zhang K, Johnson JR, Karvan O, Koros WJ. Unexpected molecular sieving properties of zeolitic imidazolate framework-8. *J Phys Chem Lett*. 2012;3(16):2130–2134.
51. Merkel TC, Bondar VI, Nagai K, Freeman BD, Pinnau I. Gas sorption, diffusion, and permeation in poly(dimethylsiloxane). *J Polym Sci Part B: Polym Phys*. 2000;38(3):415–434.
52. Tanaka K, Taguchi A, Hao J, Kita H, Okamoto K. Permeation and separation properties of polyimide membranes to olefins and paraffins. *J Membr Sci*. 1996;121(2):197–207.
53. Liu J. Development of next generation mixed matrix hollow fiber membrane for butane isomer separation, Ph.D. Dissertation, Georgia Institute of Technology in Atlanta, Georgia, USA, 2010.
54. Esekhile O. Mixed matrix membranes for mixture gas separation of butane isomers, Ph.D. Dissertation, Georgia Institute of Technology in Atlanta, Georgia, USA, 2011.
55. Henis JMS, Tripodi MK. Composite hollow fiber membranes for gas separation: the resistance model approach. *J Membr Sci*. 1981;8(3): 233–246.
56. Ekiner OM, Vassilatos G. Polyaramide hollow fibers for hydrogen/methane separation-spinning and properties. *J Membr Sci*. 1990; 53(3):259–273.
57. Li K, Olson DH, Seidel J, Emge TJ, Gong H, Zeng H, Li J. Zeolitic imidazolate frameworks for kinetic separation of propane and propene. *J Am Chem Soc*. 2009;131(30):10368–10369.
58. Pan Y, Li T, Lestari G, Lai Z. Effective separation of propylene/propane binary mixtures by ZIF-8 membranes. *J Membr Sci*. 2012;390–391:93–98.
59. Liu D, Ma X, Xi H, Lin YS. Gas transport properties and propylene/propane separation characteristics of ZIF-8 membranes. *J Membr Sci*. 2014;451(0):85–93.
60. Hara N, Yoshimune M, Negishi H, Haraya K, Hara S, Yamaguchi T. Diffusive separation of propylene/propane with ZIF-8 membranes. *J Membr Sci*. 2014;450(0):215–223.

Manuscript received Mar. 6, 2014, and revision received Apr. 15, 2014.